Wind Tunnel Testing of Novel Wing Configurations for Design and Customisation in an Industry 4.0 Environment

Jimeng Yang, Konstantinos Kontis,Yun Li*
School of Engineering
University of Glasgow
Glasgow G12 8LT, United Kingdom
j.yang.4@research.gla.ac.uk,kostas.kontis@glasgow.ac.uk, *Corresponding author: Yun.Li@glasgow.ac.uk

***Abstract*—Industry 4.0 calls for validated simulations for rapid customization and through-life designs. Wind tunnel experiments are widely used in validating flow-field simulations for aircraft design and manufacture. In this paper, we develop testing for simulating the NACA0015 model wings in various shapes and Angles of Attacks (AoA) through an anatomy wind tunnel. Particle traces are recorded during the tests and then analyzed with PIVlab and Tecplot for validating streamlines and vorticity distributions. The experimental results show that the wing shape with a relatively large angle of sweepback and an AoA ranging from +10to +15deg possess good aerodynamic behaviors for an aircraft. We discuss future prospects of aircraft simulations in an Industry 4.0 context.**

Keywords—Wind Tunnel, wing, Angle of Attack, streamline, vorticity, flow separation, laminar, turbulent, leading-edge vortex, Industry 4.0

I. INTRODUCTION

In aircraft design, an optimized configuration of novel wing for long-endurance aircraft helps achieve high lift, low induced drag and heavy weight-loading capacities.[1]In order to test these aerodynamic behaviors of a design simulations and customization in an Industry 4.0 context, both fluid dynamic analysis and model experiments are necessary. Industry 4.0, or the 'fourth industrial revolution', refers to the current trend of automation in manufacturing technologies involving cyber-physical systems.[2]

Since the 19th century, wind tunnel experiments have become an essential testing technology in a considerable part of scientific research domains, such as automobiles, aviations, meteorologists, architectures and so on. By utilizing other required auxiliary devices, the wind tunnel testing is able to simulate and analyze both laminar and turbulent distributions in the boundary layer.[3][4]From the results engineers can optimize the design for dampening the airflow separation and induced drag generation. The experiment discussed in this paper has utilized the same approach to test three novel wing configurations.

II. EXPERIMENT CONTENT AND APPARATUS

A. *ExperimentalContent*

The basic content of this experiment was to utilize NACA0015 model wings to simulate and record the airflow condition in wind tunnel. Three model wings employed in this project were triangular, square and circular shape, which were designed through CAD software Solidworks and then manufactured through 3D printing. The material was general plastic. During the experimental stage, each model wing was respectively mounted in the wind tunnel test section while the AoA was varied from 0deg to +22deg. Meanwhile, the PIV (Particle Image Velocimetry) software was operated to capture the motion of airflow over the upper surface and leading edge of the model wings. During the result analysis stage, the images were processed through the PIVlab and Tecplot software for obtaining the distribution maps of streamlines and vorticities. Finally, the optimal wing and a suitable AoA could be selected through the result comparison and analysis.

B. *Resources Required*

a) *Model Wings*

The model wings employed in this experiment were designed as simple airfoil shapes. The reason was it was difficult to simulate the flow field around a three-dimensional shape due to the complex flow conditions when the Reynolds number is low.[2]In order to uniform the variables, all model wings were designed with the same vertical length (as shown in Figure 1,2,3) and same symmetrical NACA0015 cross-section due to its good aerodynamic performance (as shown in Figure 4). In addition, each model was sprayed with black paint for reducing the laser reflection during the experiment.

b) *Anatomy Wind Tunnel*

The wind tunnel employed in this experiment was the low-speed straight-flow closed test-section wind tunnel (as shown in Figure 5), providing straight and low speed wind from the contraction section to the diffuser section. The specifications and parameters are shown as follows,

Test section: 4ft × 3ft (1.15m × 0.95m)
Maximum speed: 30m/s (65mph)
Reynolds Number: 2.50×10^5

The Reynolds number of wind tunnel is calculated as the following equation [5],

$$Re = \frac{\rho v d}{\mu}$$

where d = 173.2mm is the vertical length of three model wings, v = 20 m/s is the free stream velocity, ρ = 1.29kg/m^3 is the average air density, $\mu = 1.79\times10^5 Pa\cdot s$ is the coefficient of air viscosity under the standard atmospheric pressure. Above all, it derives that the Reynolds Number Re= 2.50×10^5.

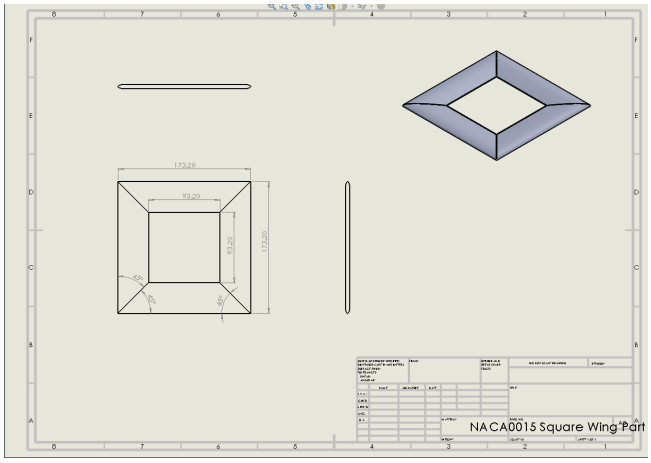

Fig. 1.Orthographic Views of Square Wing

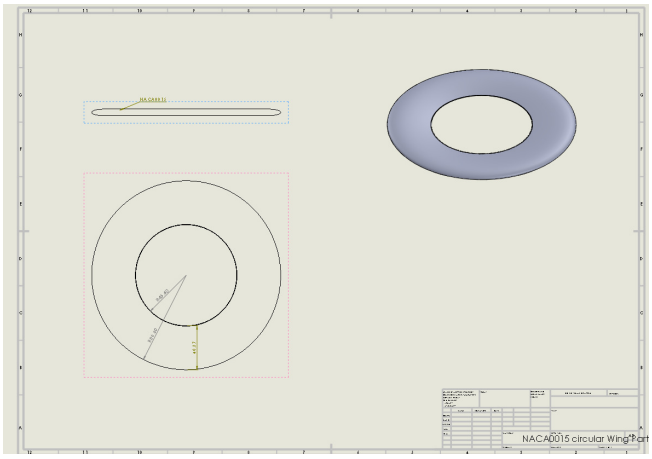

Fig. 2.Orthographic Views of Circular Wing

c) *Other Resources*

1. Laser(Class 4) for the PIV System

The class 4 laser located above the test section provided a planar laser to illuminate the smoke particles around model wings in a dark condition. The intensity of laser was set to the maximum value of 10 degree for obtaining clear particle images.

2. Smoke Oil

The smoke oil provided an appropriate amount of smoke with micrometer-sized particles from contraction section to diffuser during the experiment. The traces of particles could represent the airflow track around model wings.

3. PIV (Particle Image Velocimetry)

The PIV connected with the camera was operated to capture the particle images during the experiment.

4. PIVlab Software

The PIVlab was able to select available parts of particle images and generate the velocity vector of each pixel point in the form of distribution maps.

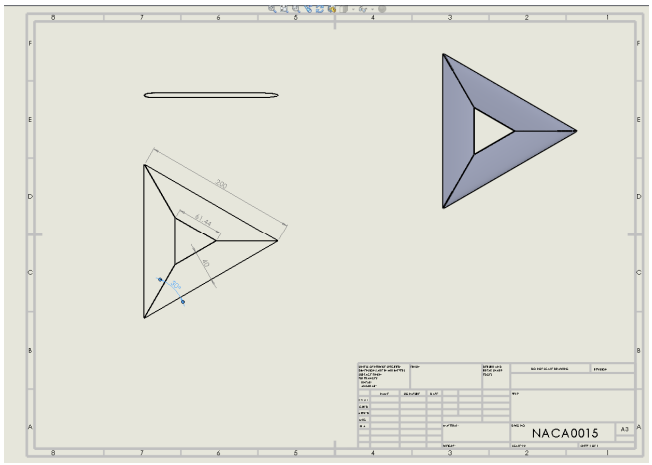

Fig. 3.Orthographic Views of Triangular Wing

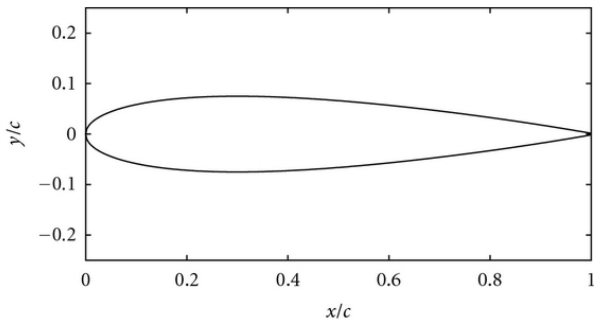

Fig. 4. Cross Section of NACA0015 [6] *.c* is the chord of NACA0015 wing. *x/c* and *y/c* are the ratio of *x* and *y* to the chord length *c* respectively.

5. Tecplot Software

The Tecplot was used to generate the distribution maps of vorticities of the airflow around model wings in different AoA.

III. METHODOLOGY

A. AoA Selection

The selecting range of AoA was limited due in part to the plastic material of models. During the experiments, it was observed that the obvious vibration occurred in high AoA, especially for the square wing. Thus, the range of AoA was selected from 0deg to +22deg.

In order to obtain an obvious difference between low and high angles, the low AoA were thus set to 0deg and +2deg. High AoA were set to 10deg as interval, which were +12deg and +22deg respectively.

B. Model Observation Range

Due to the limitation of laser irradiation range, the laser light could only irradiate the upper surface of models leading to a shadow generation under the lower surface. Thus, the observation range was selected as the combination of upper surface and leading edge.

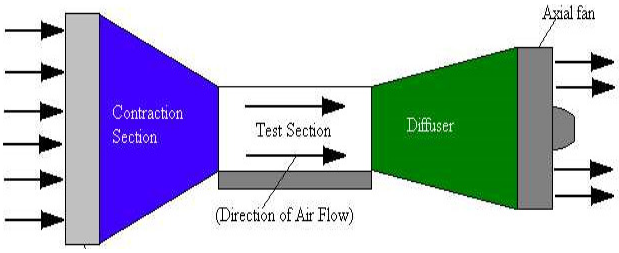

Fig. 5.Straight-flow Closed Wind Tunnel [7]

C. Setting of PIV

Shortening the time of image capture was necessary due to the smoke dissipation. Based on the configuration of camera, the interval time between each pair of images was knows as 50 microseconds. In order to ensure all images could be captured in limited time and most particle traces were clear and regular, the number of images was thus set to 25 pairs per test. In addition, for ensuring the accuracy of experimental results, each angle was required to be tested for 4 times. Above all, the total number of images for each angle was set to 100 pairs.

D. Wind Speed

The units of wind speed required to be converted from meters per second (m/s) to millimeters water column (mmH_2O). Thus, the calculation of wind speed was expressed as follows,

1). The Bernoulli's Equation of steady airflow can be written,

$$\frac{1}{2}\rho v^2 = K\Delta P \tag{1}$$

where ρ is the air fluid density, v= 20m/s is the wind speed, K = 1.237, ΔP is the pressure difference.

2). Pressure difference,

$$\Delta P = \rho_{H_2O} g \Delta H_2O \tag{2}$$

where ρ_{H_2O} is the water density, g is the acceleration of gravity, ΔH_2O is the water-column height.

3). Thermodynamic temperature [8],

$$T = t + 273.15 \tag{3}$$

where t is the centigrade temperature.

4). Ideal gas low,

$$P = \rho RT \tag{4}$$

where $R = 287 kg/J \cdot m^3$ is the gas constant.

5). Atmospheric pressure could be also expressed as,

$$P = \rho_M g \Delta h_M \tag{5}$$

where $\rho_M = 13.6 \times 10^3 kg/m^3$is the mercury density, Δh_M is the height of mercury column.

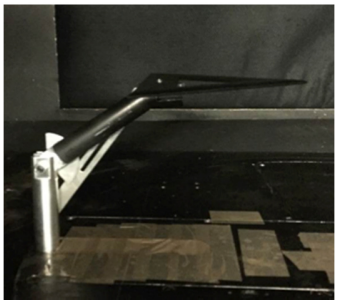

Fig. 6. Model Installation

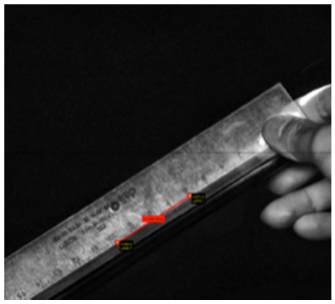

Fig. 7. Calibration

From (4) and (5), the air density could be derived as,

$$\rho = \frac{\rho_M g \Delta h_M}{RT} \tag{6}$$

Then by substituting (2) and (6) into (1), the equation of the water-column height (ΔH_2O) and wind speed (v) could be expressed as,

$$\Delta H_2O = \frac{v^2 \Delta h_M}{52.21T}$$

The degrees of centigrade temperature (t) and the height of mercury column (Δh_M) required to be recorded each test due to the variable atmospheric condition.

IV. Procedure

A. Model Installation

As shown in Figure 6, the model wing was fixed on the bracket in the test section of wind tunnel. The direction of the model centerline was parallel to the airflow direction.

B. Image Capture

After setting the wind speed to 20m/s and the laser intensity to maximum degree, an appropriate amount of smoke was released. By operating the PIV, the particle images were then captured by camera in a clear condition.

The interval time between each pair of images was 50 microseconds. Thus the distance of particle's movement in each pair of images was 1 meter approximately.

C. Calibration

In order to unify the length in images and actual condition, it was necessary to capture the image of ruler under the same testing condition after each test (as shown in Figure 7).

V. Results and Discussioons

A. Streamlines

The PIVlab software is able to depict the streamlines and calculate the velocity of particle motions in each pair of images.

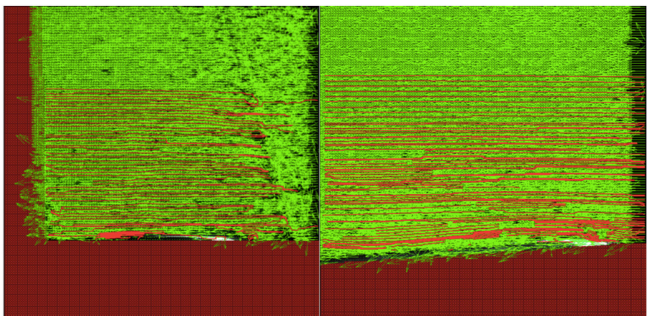

Fig. 8.Streamline of Low AoA around Triangular Wing

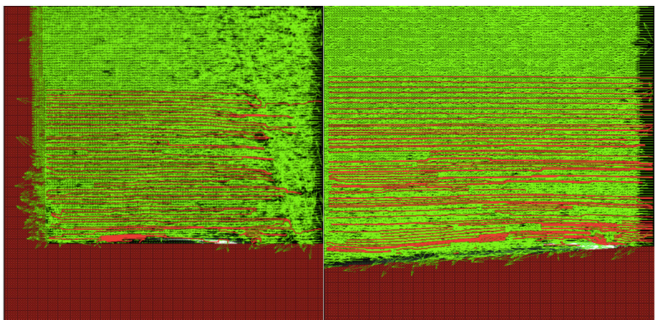

Fig.9.Streamline of High AoA around Triangular Wing

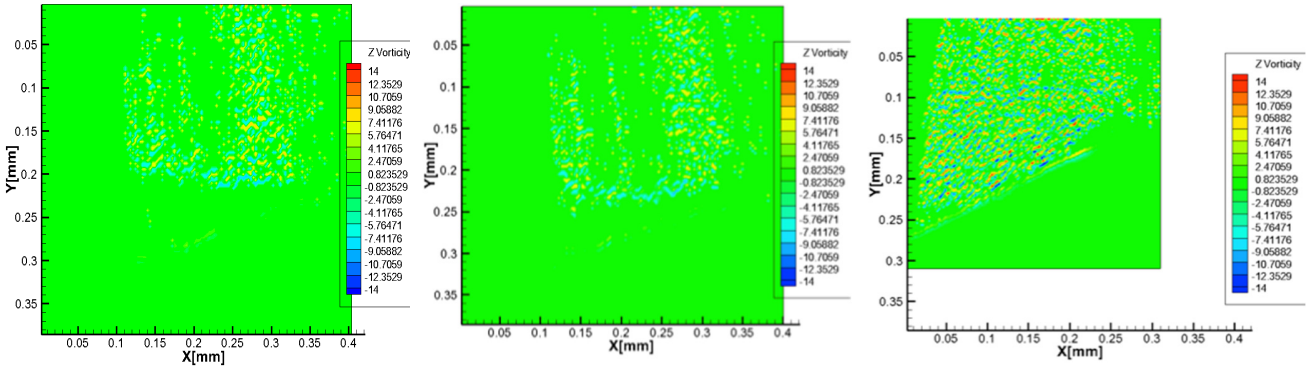

(a) Square Wing (b) Circular Wing (c) Triangular Wing

Fig.10. Vorticity Magnitudes in +22deg

According to the results of PIVlab, the streamlines are generated as fluent curves distributed around the model wing. For example of triangular wing (as shown in Figure 8), it is observed that the streamlines are steadily distributed as boundary layers attaching to the upper surface in low AoA such as 0deg and +2deg. This flow state is regarded as laminar resulted from the viscous properties of fluid. [9]

In contrast, as AoA increasing to +12deg and +22deg, the streamlines are distributed in instable and irregular state over the trailing edge, which are described as turbulent flow. As shown in Figure 9, the velocity vectors of particle motions constantly change in magnitudes and directions. [10] This turbulent flow is resulted from the airflow separation, which generally occurs in high AoA.

The explanation is the boundary layer may continue flowing backward until the flow velocity against the adverse pressure gradient drops to zero. Thus the airflow is unable to adhere to the upper surface and the streamlines are unable to maintain coherence, causing the airflow separation and turbulent flow generation near the trailing edge. Generally, the higher of the AoA, the earlier airflow separation occurs.[11]

In aerodynamic field, the airflow separation may result in drag generation as it can significantly change the flow-field condition from inviscid to strong viscid when the Reynolds number is high.[12] For this reason the improvement and optimization of airfoil design are required for achieving separation delay and longer flow attaching time.

B. Vorticity Distribution

The Tecplot Software is able to generate the distribution map of vorticity based on the mean velocity obtained from the PIVlab.

According to the comparison of vorticity magnitudes in a same AoA (as shown in Figure 10), it is observed that the vorticities are intensively distributed from the leading edge to 70 percent chord position, which are described as the leading-edge vortexes (LEV). The LEV is formed through the rolling up of vorticity layers resulted from the fluid viscosity and airflow separation around the leading edge. [13]

In aerodynamic field, the LEV is a necessary role for enhancing vortex-induced lift, especially for high sweep-angle or low aspect ratio structure such as delta wing.[14][15]The explanation is the vortex sheet from the trailing edge is continuously added to the vorticities on the swept leading edge, gradually forming an increased LEV on the upper surface. Thus it can be observed from the results that the maximum vorticity of triangular wing is twice of other two wings. For example of +22deg (as shown in Figure 10), the maximum vorticity of the triangular wing is $21.4s^{-1}$ while the values of other two wings are both around $14.0s^{-1}$. In addition, higher LEV may induce higher lift. Due to the high velocity magnitude in the core of a LEV, the low static pressure and high vortex-induced lift are formed in this area. Above all, it indicates that the triangular wing has better aerodynamic

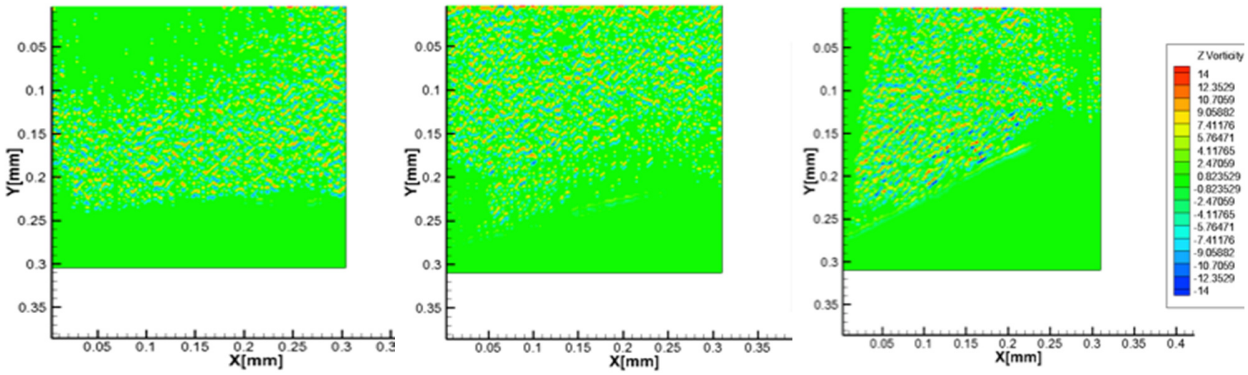

(a) +2deg (b) +12deg (c) +22deg

Fig.11. Vorticity Magnitudes of Triangular Wing

advantages than other structures based on its high vortex and high-induced lift characteristics.

Despite the induced lift, the drag is generated as well. For a thin airfoil, the lift may proportionally increase as the AoA rises in the range of small AoA (from -10deg to +10deg). However, when the AoA is high, the drag may sharply increase resulted from the airflow separation. The turbulent flows generated in the separated location may lead to the wing stall and unsteady drag.

As shown in Figure 11, it is observed that the vorticity of the same wing increases as the AoA rises. For achieving both high lift and low drag, the suitable AoA for thin or low aspect ratio airfoils should be from +10deg to +15deg [16].

C. *Test Limitations*

Although the results coincide with the law of physics, there still exists a few limitations of the wind tunnel test.

a) *Plastic Material*

The AoA range is limited due to the general plastic material of model wings. Different with aluminum alloy or other composite materials, the general plastic is comparatively fragile resulting in the strong vibration in large AoA such as +30deg of the square wing in this experiment.

b) *Complexity*

Before each test beginning, the centigrade temperature (t) and the height of mercury column (Δh_M) required to be measured due to the variable atmospheric state, resulting in a large number of data calculation. In addition, the quality of the test result is also affected by the density of particles. However, the accurate amount of smoke release is difficult to control. For this reason the experimental replications has consumed plenty of time.

c) *Observation Range*

During the experiment, the laser could only illuminate the upper surface and leading edge. Thus it is infeasible to test and analyze the flow motion on the lower surface.

Above all, it indicated that the manual operation is always accompanied with the generation of errors or limitations. To improve the test technology for achieving more accurate and comprehensive results, the virtualized test instruments are required to be developed and replace the existing approach.

VI. Conclusions and Future Work

A. *Conclusion*

This paper has developed wind tunnel tests for simulations of three model wings with the NACA0015 symmetrical cross section in various shapes and AoAs. Through the comparison and analysis of the testing results, the conclusion can be summarized in two points.

1) A wing with a relatively large sweepback-angle structure, such as the delta or triangular wing, possesses good aerodynamic characteristics for enhancing high vortex-induced lift.

2) An angle from +10 to +15deg is a suitable AoA range for achieving both a high lift and an airflow separation delay.

B. *Future Work*

At present, simulation for customization and testing for aircraft design are continuously developing and innovating. [17]New technologies to realize entire validation tests for not only an aircraft but also any customized products are required for future industrial design and manufacture, especially in the context of Industry 4.0.

Although the development of Industry 4.0 is still in the initial phase, 3D simulations and test of product designs, materials, and production processes have already been applied in relevant domains. Utilization of real-time data to merge physical objects with the virtual world is a principle research area. For example, product lifecycle management (PLM) from Siemens has enabled a virtual machine to simulate, develop and test the product or components by using data obtained from a physical machine. [18][19] It is believed that engineers can spend more time in the virtual world rather than the real world in the future. [20] With validated flow-field simulations around, smart factories can be built for space vehicles too.

REFERENCES

[1] Austin, R. (2010). Unmanned air vehicles. Chichester, West Sussex, U.K.: Wiley, pp.45-47

[2] Wikipedia, "Industry 4.0",https://en.wikipedia.org/wiki/Industry_4.0, accessed October 2016.

[3] Varshney, Kapil, and Kamal Poddar. "Experiments on integral length scale control in atmospheric boundary layer wind tunnel." Theoretical and applied climatology 106.1-2 (2011): 127-137.

[4] Al-Quraan, Ayman, Ted Stathopoulos, and Pragasen Pillay. "Comparison of wind tunnel and on site measurements for urban wind energy estimation of potential yield." Journal of Wind Engineering and Industrial Aerodynamics 158 (2016): 1-10.

[5] Dwivedi, P. Nfffe, and S. N. Upadhyay. "Particle-fluid mass transfer in fixed and fluidized beds." Industrial & Engineering Chemistry Process Design and Development 16.2 (1977): 157-165.

[6] Carrigan, Travis J., et al. "Aerodynamic shape optimization of a vertical-axis wind turbine using differential evolution." *ISRN Renewable Energy* 2012 (2012), pp.9-10

[7] Seniordesign. (2016). Housing & Framework Decisions. [online] Available at: https://seniordesign.engr.uidaho.edu/1999_2000/airteam/duct.html [Accessed 16 Mar. 2016].

[8] Ifisc.uib-csic.es. (2016). [online] Available at: http://ifisc.uib-csic.es/raul/CURSOS/TERMO/Thermodynamic%20temperature.pdf [Accessed 25 Oct. 2016].

[9] Howarth, L. "Laminar boundary layers." *Fluid Dynamics I/Strömungsmechanik I*. Springer Berlin Heidelberg, 1959. 264-350.

[10] Andersson, Bengt, et al. "Turbulent-Flow Modelling." *Computational Fluid Dynamics for Engineers:*. Cambridge: Cambridge University Press, 22 Dec. 2011. 62–112. Web.

[11] Community.dur.ac.uk. (2016). [online] Available at: https://community.dur.ac.uk/suzanne.fielding/teaching/BLT/sec4c.pdf [Accessed 15 Oct. 2016].

[12] Rhie, C. M., and W. L. Chow. "Numerical study of the turbulent flow past an airfoil with trailing edge separation." *AIAA journal* 21.11 (1983): 1525-1532.

[13] Earnshaw, PBi. An experimental investigation of the structure of a leading-edge vortex. HM Stationery Office, 1962.

[14] Shyy, Wei, and Hao Liu. "Flapping wings and aerodynamic lift: the role of leading-edge vortices." *AIAA journal* 45.12 (2007): 2817-2819.

[15] Polhamus, Edward C. "A concept of the vortex lift of sharp-edge delta wings based on a leading-edge-suction analogy." (1966).

[16] Dickinson, Michael H., and Karl G. Gotz. "Unsteady aerodynamic performance of model wings at low Reynolds numbers." *Journal of Experimental Biology* 174.1 (1993): 45-64.

[17] Wong, K. C., H. J. H. Peters, and P. Catarzi. "Adapting to Limitations of a Wind Tunnel Test Facility in the Aerodynamic Testing of a new UAV." *9th Australian International Aerospace Congress (AIAC 2001)*. 2001.

[18] Rüßmann, Michael, et al. "Industry 4.0: The Future of Productivity and Growth in Manufacturing Industries." *Boston Consulting Group* (2015).

[19] Lee, Jay, Behrad Bagheri, and Hung-An Kao. "A cyber-physical systems architecture for industry 4.0-based manufacturing systems." *Manufacturing Letters* 3 (2015): 18-23.

[20] Anon, (2015). *quarterly journal*, 36(01 Q4 2015), pp.16-19.